Optimal coherent control of dissipative *N*-level systems

H. Jirari and W. Pötz
Institut für Theoretische Physik, Karl-Franzens-Universität Graz, Universitätsplatz 5, 8010 Graz, Austria
(Received 8 September 2004; revised manuscript received 20 December 2004; published 22 July 2005)

General optimal coherent control of dissipative *N*-level systems in the Markovian time regime is formulated within Pointryagin's principle and the Lindblad equation. In the present paper, we study feasibility and limitations of steering of dissipative two-, three-, and four-level systems from a given initial pure or mixed state into a desired final state under the influence of an external electric field. The time evolution of the system is computed within the Lindblad equation and a conjugate gradient method is used to identify optimal control fields. The influence of both field-independent population and polarization decay on achieving the objective is investigated in systematic fashion. It is shown that, for realistic dephasing times, optimum control fields can be identified which drive the system into the target state with very high success rate and in economical fashion, even when starting from a poor initial guess. Furthermore, the optimal fields obtained give insight into the system dynamics. However, if decay rates of the system cannot be subjected to electromagnetic control, the dissipative system cannot be maintained in a specific pure or mixed state, in general.

DOI: 10.1103/PhysRevA.72.013409 PACS number(s): 32.80.Qk, 03.65.Yz, 78.20.Bh, 78.67.−n

I. INTRODUCTION

In view of the prospects for data encryption, secure information transfer, enhanced computation power and related applications, the ability to coherently manipulate quantum systems in a controlled fashion has become one of the highest priorities in todays research [1]. While a substantial number of powerful quantum algorithms exist on paper, only rather basic schemes have been implemented in real systems to this day. Several important issues have to be resolved to achieve useful implementation of quantum algorithms [2]. Some of the most important practical issues are fabrication of suitable quantum systems (qubit), including controllable coupling mechanisms, scalability, and isolation. The latter is important for maintaining quantum coherence, however, frequently, conflicts with effective coupling among qubits and scalability.

In the present paper we investigate theoretically the extent to which simple dissipative quantum systems can be steered into a selected pure or mixed target state by means of an external electric field. This objective is phrased as an optimum control problem. The content of this paper is twofold: First, we develop a numerical approach to optimal control of dissipative quantum systems for a large class of cost functionals. Second, we present results regarding feasibility of optimum coherent control in the presence of dissipation when the system's dynamics can be phrased within the Lindblad equation. Recently, the Lindblad equation has been used, for example, to study optimum feedback control, quantum error correction, or laser cooling of molecules [3–6]. Here we consider primarily the objective of preparation of a dissipative quantum system in a specified target state at some specified target time. In particular, we study to what extent decoherence can be defeated by optimum coherent control.

This paper is organized as follows. In Sec. II, we formulate the optimum control problem for a general cost functional within Pontryagin's principle, and formulate the specific objective of driving the system into a selected target state. In Sec. III, we present the numerical approach in form of a conjugate gradient method. A brief review of the Lindblad equation as a quantum optical master equations is given in Sec. IV. The construction of Lindblad operators is reviewed for the dissipative two-level system. In Sec. V, we present our numerical results for "ladder-type" *N*-level systems, as well as a three-level and four-level Λ system, as used in stimulated-Raman-adiabatic-passage (STIRAP) experiments. The summary and conclusions are given in Sec. VI.

II. QUANTUM OPTIMAL CONTROL PROBLEM

A. General formulation of the problem

Optimum control theory has a long-standing tradition in various fields of physics [7]. To our knowledge, one of the first applications to a quantum system has been in the field of quantum chemistry [8]. More recently, optimum control studies have been extended to nonlinear coherent systems [9] and dissipative systems [10,11]. A variety of schemes has been proposed for quantum systems [8,12–16]. In this paper we consider the following model quantum control problem. Let time t be in $[0,T]$, for T fixed. $\rho(t)$ is the density operator acting on $\mathcal{H}=\mathbb{C}^N$, the Hilbert space of dimension N. $\rho(t)$ represents the state (density operator) of the system interacting with its environment. Making the Markov approximation for the system-environment interaction, the time evolution of a dissipative quantum system is described by a Lindblad equation of the form [17]

$$i\hbar\frac{d}{dt}\rho(t)=[H_0+H_I(\varepsilon(t)),\quad \rho(t)]+L_D[\rho(t)], \tag{1}$$

with initial condition $\rho(0)=\rho_0$, where H_0 is the internal system Hamiltonian, $H_I(\varepsilon(t))$ is the control Hamiltonian, and

$$L_D[\rho(t)] = i\hbar \sum_{\mu=1}^{N^2} \left(L_\mu \rho(t) L_\mu^\dagger - \frac{1}{2}\{L_\mu^\dagger L_\mu, \rho(t)\} \right) \tag{2}$$

is the dissipation superoperator. $L_\mu, \mu = 1 \cdots N^2$ are the Lindblad operators. As the dimension of the Hilbert space N is finite, all the operators appearing in the Lindblad equation are bounded. They are represented by $N \times N$ matrices. $\varepsilon(t) \in \mathcal{L}^2[0,T]$ is the (electric) control field. It is real valued.

The objective is formulated by means of a cost functional for which we choose the general form

$$J(\varepsilon) = \mathrm{Tr}\{\Phi_o(\rho(T))\} + \int_0^T dt\, \mathcal{L}(\rho, \varepsilon, t), \tag{3}$$

where $\mathcal{L}$ is the performance index [7],

$$\mathcal{L}(\rho, \varepsilon, t) = \mathrm{Tr}\{\Phi(\rho(t), t)\} + \frac{1}{2}\alpha(t)\varepsilon^2(t). \tag{4}$$

The functionals $\Phi_o(\rho(T))$ and $\Phi(\rho(t), t)$ are bounded from below and differentiable with respect to $\rho(T)$ and $\rho(t)$, respectively. They account for the specific objective at target time T and intermediate times $t \in [0,T)$. They are examples for what has been termed final cost functional and running cost functional in the literature [7]. The third contribution to the cost functional J penalizes large control fields. It is required to make the problem well posed [8]. $\alpha(t)$ is a given (real-valued) function of time which determines the relative importance of the third contribution at time t. In the simplest case, it may be a constant. As will be shown below, it may be used to force the control field to approach zero near the end points of the time interval in accordance with experiment where light fields are of finite duration. An optimum control field is one which minimizes the cost functional.

B. Formulation within Pontryagin's principle

Consider the quantum optimal control problem of minimizing the functional (3) subject to the dynamical constraint (1). An optimal solution of this problem is characterized by first-order optimality conditions in the form of the Pontryagin's minimum principle [7,18,19]. These conditions are formulated with the the help of the Hamilton function that has the following form in our problem:

$$\mathcal{H}(\rho, \varepsilon, \lambda) := \mathcal{L}(\rho, \varepsilon, t) + \mathrm{Tr}\left\{ \frac{\lambda(t)}{i\hbar}[H, \rho(t)] + L_D[\rho(t)] \right\}, \tag{5}$$

with $H = H_0 + H_I$. The matrix λ is called the adjoint state. Pontryagin's minimum principle states that a necessary condition for (ρ, ε) to be a solution of the above optimal control problem is the existence of an adjoint state λ such that

$$\begin{cases} \dfrac{d}{dt}\rho(t) = \dfrac{\partial \mathcal{H}(\rho(t), \varepsilon(t), \lambda(t))}{\partial \lambda(t)}, & t \in [0,T] \\ \dfrac{d}{dt}\lambda(t) = -\dfrac{\partial \mathcal{H}(\rho(t), \varepsilon(t), \lambda(t))}{\partial \rho(t)}, & t \in [0,T] \\ \rho(0) = \rho_i, \quad \lambda(T) = \Phi'_o(\rho(T)) \\ 0 = \dfrac{\partial \mathcal{H}(\rho(t), \varepsilon(t), \lambda(t))}{\partial \varepsilon(t)}, & t \in [0,T], \end{cases} \tag{6}$$

where $\Phi'_o(\rho(T)) \equiv \delta\Phi_o / \delta\rho(T)$. The stationarity conditions (6) are derived in the Appendix. Sufficient conditions for a "local minimum" with respect to the control ε are the optimality condition

$$\frac{\partial \mathcal{H}(\rho(t), \varepsilon(t), \lambda(t))}{\partial \varepsilon(t)} = 0, \tag{7}$$

and

$$\frac{\partial^2 \mathcal{H}(\rho(t), \varepsilon(t), \lambda(t))}{\partial \varepsilon^2(t)} > 0. \tag{8}$$

If $\partial^2\mathcal{H} / \partial\varepsilon^2 \neq 0$, the implicit function theorem states that the relation (7) is equivalent to

$$\varepsilon = \varepsilon(\rho(t), \lambda(t)). \tag{9}$$

The differential system (6) is thus equivalent to the differential system with differential variables (ρ, λ),

$$\begin{cases} \dfrac{d}{dt}\rho(t) = \dfrac{\partial \mathcal{H}(\rho(t), \varepsilon(\rho(t), \lambda(t)), \lambda(t))}{\partial \lambda(t)}, & t \in [0,T] \\ \dfrac{d}{dt}\lambda(t) = -\dfrac{\partial \mathcal{H}(\rho(t), \varepsilon(\rho(t), \lambda(t)), \lambda(t))}{\partial \rho(t)}, & t \in [0,T] \\ \rho(0) = \rho_i, \quad \lambda(T) = \Phi'_o(\rho(T)). \end{cases} \tag{10}$$

In this form, the quantum optimal control problem is equivalent to a two-point boundary value problem. It is extremely difficult to solve because of the apparent nonlinearity in the system of differential equations (10).

For the general cost functional (3) and the Lindblad equation (1) the necessary conditions for an extremum (6) take the following form:

(i) $\rho(t)$ with $0 \leqslant t \leqslant T$ is the state variable and the solution of the Lindblad equation (1).

(ii) The adjoint-state variable is the solution of the differential equation

$$i\hbar \frac{d}{dt}\lambda(t) = [H_0 + H_I(\varepsilon(t)), \lambda(t)] + L_D^\dagger[\lambda(t)] + \Phi'(\rho(t)). \tag{11}$$

(iii) The optimally condition for the external field $\varepsilon(t)$, regardless of the specific form of the cost functional, is

$$\alpha(t)\varepsilon(t) + \mathrm{Tr}\left\{ \frac{\lambda(t)}{i\hbar}\left[\frac{\partial H_I(\varepsilon(t))}{\partial \varepsilon(t)}, \rho(t) \right] \right\} = 0. \tag{12}$$

Equation (12) is obtained after integration of the adjoint-system Eq. (11) backward in time which is a backward-time linear Cauchy problem. Note that from its initial condition at $t=T$ it is clear that the adjoint-state matrix $\lambda(t)$, in general, cannot be interpreted as a density matrix. The variation of the cost functional (3) is given by

$$\frac{\delta J}{\delta \varepsilon(t)} = \int_0^T \frac{\partial \mathcal{H}}{\partial \varepsilon} dt = \int_0^T dt \left(\alpha(t)\varepsilon(t) + \mathrm{Tr}\left\{ \frac{\lambda(t)}{i\hbar} \left[\frac{\partial H_I(\varepsilon(t))}{\partial \varepsilon(t)}, \rho(t) \right] \right\} \right). \tag{13}$$

In summary, the prescription is as follows: select an initial guess for the control field $\varepsilon(t)$ and compute $\rho(t)$ by integration forward in time. Use $\rho(T)$ in the initial condition for the computation of $\lambda(t)$ backward in time. Use Eq. (12) to update the electric field, as detailed below, and run through this loop until convergence is reached.

C. Specification of the cost functional for final-state selection

In this work, we consider one specific objective: control of the system evolution from a given initial state $\rho(0)$ into a desired final state at specified $T \geqslant 0$ when the system starts in a given initial state. It may be desirable to prepare a quantum system in a specific (pure or mixed) state ρ_T for various reasons. For example, one may wish to ionize an atom or molecule, initiate a certain molecular dissociation, prepare a qubit, transfer an electron from one state of a quantum dot into another, etc. In this case, we need to minimize the deviation of the state of the system at final time $\rho(T)$ from the desired state ρ_T. For the cost functional we choose

$$\mathrm{J} = \frac{1}{2}\|\rho(T) - \rho_T\|_F^2 + \frac{1}{2}\int_0^T \alpha(t)\varepsilon^2(t)dt. \tag{14}$$

Here, $\Phi(\rho(t))=0, t \in [0,T]$ and

$$\mathrm{Tr}\{\Phi_o(\rho(T))\} = \frac{1}{2}\|\rho(T) - \rho_T\|_F^2, \tag{15}$$

where ρ_T is the target density matrix and $\|\cdot\|_F$ is the Frobenius norm.[1] This cost functional requires $\lambda(T)=\rho(T)-\rho_T$ as the initial condition in Eq. (11) for the backward integration of the adjoint state variables $\lambda(t)$.

III. NUMERICAL ALGORITHM

A. Introduction

There are two main approaches for solving optimal control problems [19]. The so-called indirect method, based on Pontryagin's minimum principle, constructs the Hamiltonian and adjoint system corresponding to a given optimal control problem and then solves the resulting boundary value problem for the optimal control field. The latter is to be determined throughout the time interval $[0,T]$. In the direct method, the control field is parametrized in a lower dimensional space and the resulting nonlinear problem is solved directly.

In the present work we implement a version of the gradient method. More precisely, the optimization is performed using the gradient method with the step length chosen by a line search technique which is based on a minimization rule followed by the conjugate gradient method with Poalk-Ribiere update of the search direction [21].

B. Gradient method

Gradient methods represent the most frequently used approach for solving an optimal control problem [7,8,21]. They are characterized by iterative algorithms for improving estimates of the control histories, $(\rho(t),\varepsilon(t))$, so as to come closer to satisfying the optimally and boundary conditions. An obvious advantage of this approach over, for example, the shooting method is that any guess $\varepsilon_i(t)$ for the control field will produce manageable values for the state $\rho(t)$ during integration regardless of initial conditions. The resulting value $\rho(t)$ can be used to integrate the co-state equation backward in time, providing an approximation of the state-adjoint-state trajectory $(\rho(t),\lambda(t))$ consistent with $\varepsilon_i(t)$. Since in general ε_i will be different from an optimal control field, an iteration scheme which provides convergence must be employed. Gradient methods use the gradient information for the cost functional to obtain $\varepsilon_{i+1}(t)$ such that $\varepsilon_i(t)$ converges to an optimal solution as $i \to \infty$ [7].

Numerical solution of the optimal control problem is difficult as, in principle, it involves the determination of the control field $\varepsilon(t)$ at an infinite number of mesh points in the time interval $I=[0,T]$. In order to find a numerical solution of the problem, we convert the infinite-dimensional problem into a finite-dimensional optimization approximation [7,21]. For this purpose, we first discretize I into M equal-sized subintervals ΔI_k with $I=\cup_{k=1}^{M}\Delta I_k$ and then approximate $\varepsilon(t)$ as $\varepsilon(t) \to \varepsilon(t_k)=\varepsilon_k$, $k=1\cdots M$. Thus the problem becomes that of finding $\varepsilon=[\varepsilon_1,\varepsilon_2,\varepsilon_3,\ldots,\varepsilon_M]^T$ such that

$$J(\varepsilon) = \inf_{\zeta \in \mathbb{R}^M} J(\zeta). \tag{16}$$

As the cost functional now depends on $\varepsilon_1,\varepsilon_2,\varepsilon_3,\ldots,\varepsilon_M$, we define the gradient of the cost functional by

$$G = \left[\frac{\partial J}{\partial \varepsilon_1}, \frac{\partial J}{\partial \varepsilon_2}, \ldots, \frac{\partial J}{\partial \varepsilon_M} \right]^T, \tag{17}$$

where

$$\frac{\partial J}{\partial \varepsilon_k} = \frac{1}{\Delta \varepsilon_k}[J(\varepsilon_1,\varepsilon_2,\ldots,\varepsilon_k+\Delta\varepsilon_k,\ldots,\varepsilon_N) - J(\varepsilon_1,\varepsilon_2,\ldots,\varepsilon_k,\ldots,\varepsilon_N)]. \tag{18}$$

We have, by applying the Riemannn-rule integration scheme to Eq. (13),

[1] Given a matrix $n \times nA=a_{ij}$, $\|A\|_F^2=\Sigma_{ij}|a_{ij}|^2=\Sigma_{ij}a_{ij}a_{ij}^*=\mathrm{Tr}(AA^\dagger)$ [20].

$$\frac{\partial J}{\partial \varepsilon_k} = \left(\alpha_k \varepsilon_k + \mathrm{Tr}\left\{ \frac{\lambda_k}{i\hbar} \left[\frac{\partial H_{int}(\varepsilon_k)}{\partial \varepsilon_k}, \rho_k \right] \right\} \right) \Delta t_k, \qquad (19)$$

where ρ_k and λ_k are, respectively, the solution of the Lindblad equation and the adjoint system corresponding to time subinterval ΔI_k. $|\Delta I_k| = \Delta t_k$ is the length of the subinterval ΔI_k. With the gradient obtained, the following type gradient algorithm determines the optimal value of ε based on the Polak-Ribiere method [7,19,21,22]:

1. Choose the initial control field ε_0. Solve the state and adjoint systems and compute $G(\varepsilon_0)$. If $G(\varepsilon_0)=0$, stop here. ε_0 is the solution of the problem. Otherwise go to step 2.
2. Set the first searching direction $S_0 = -G(\varepsilon_0)$.
3. Set $\varepsilon_1 = \varepsilon_0 + \beta_0 S_0$, with β_0 being the optimal step length in the searching direction S_0. Set $i=1$ and go to step 4.
4. Find $G(\varepsilon_i)$ by solving the state and adjoint systems and then set $S_i = -G(\varepsilon_i) + \gamma_i S_{i-1}$, with $\gamma_i = \{([G(\varepsilon_i) - G(\varepsilon_{i-1})]G(\varepsilon_i)\}/[G(\varepsilon_{i-1})G(\varepsilon_{i-1})]$.
5. Compute the optimum step length β_i in the searching direction S_i and update $\varepsilon_{i+1} = \varepsilon_i + \beta_i S_{i+1}$.
6. Test the optimality of ε_{i+1}. If ε_{i+1} is the optimum, stop the process. Otherwise, set $i = i+1$ and go to step 4.

C. Discretization of the adjoint-state system

To determine the gradient of the cost functional, we have to solve the Lindblad equation for $\rho(t)$ and then the co-state equation for $\lambda(t)$. Both, equations are initial value problems. Various numerical methods based on standard time stepping schemes, such as the Crank-Nicholson procedure or Runge-Kutta can be used to solve the Lindblad equation and the associated adjoint system. In the present work, the discretization of the adjoint-state system is done by the classical $\frac{4}{5}$ order explicit Runge-Kutta-Fehlberg method [23]. Once the initial conditions are specified, the values of $\rho_k = \rho(t_k)$ and $\lambda_k = \lambda(t_k)$ are evaluated at every discrete time $t_k = k\Delta t_k$, $k = 1 \cdots M$.

IV. QUANTUM OPTICAL MASTER EQUATION

The interaction of matter with electromagnetic radiation in the quantum optical limit provides a typical field for the application of the Lindblad equation. We use this physical situation as an example to show how Lindblad operators can be constructed from a microscopic model for the environment. However, the same formalism is applicable to a multitude of bipartite systems, provided that the Markov approximation holds for the system-system interaction [24,25]. The radiation field represents a reservoir with infinite degrees of freedom which interacts with a quantum bound system, such as an atom, a molecule, or a quantum dot. The Hamiltonian describing the interaction between the physical system and the radiation field in the dipole approximation is given by $H_I = \vec{D} \cdot \vec{E}$, where the $\vec{D}$ is the dipole operator of the system under consideration and $\vec{E}$ is the electric-field operator. Represented in the Schrödinger picture, H_I is an operator on the Fock space $\mathcal{F} = \mathcal{H}_S \otimes \mathcal{F}_E$ of basis $|n\rangle \otimes |n_{k\lambda}\rangle$ ($\vec{k}$ and $\lambda = 1, 2$ are, respectively, the photon wave vector and its polarization). In the rotating-wave approximation, the Markovian quantum master equation describing the evolution of the physical system has the Lindblad form [24,25]

$$i\hbar \frac{d}{dt}\rho(t) = [H_S, \rho] + i\hbar \sum_{\mu,\omega>0} \Gamma(\omega) \left(L_\mu(\omega) \rho L_\mu^\dagger(\omega) - \frac{1}{2}\{L_\mu^\dagger(\omega) L_\mu(\omega), \rho\} \right), \qquad (20)$$

where H_S is the Hamiltonian of the physical system and $\Gamma(\omega)$ is the Fourier transforms of the correlation functions of the electric-field operator

$$\Gamma(\omega) = \frac{1}{\hbar^2} \int_0^{+\infty} dt\, e^{i\omega t} \langle E(t) E(0) \rangle. \qquad (21)$$

The imaginary part of $\Gamma(\omega)$ leads to a renormalization of the system Hamiltonian which is induced by the vacuum fluctuation of the radiation field (Lamb shift). Its real part leads to two types of dissipation, namely, a population relaxation (decay of the diagonal elements of the density matrix) and phase decoherence (decay of the off-diagonal elements of the density matrix). At zero temperature

$$\Gamma(\omega) = \frac{1}{2}\gamma(\omega), \quad \gamma(\omega) = \frac{1}{4\pi\epsilon_0} \frac{4\omega^3 |\vec{d}|^2}{3\hbar c^3}, \qquad (22)$$

where $\vec{d}$ is the matrix element of the dipole moments operator. Thus the Lindblad operators $L(\omega)$ describe spontaneous emission which occurs with rate $\gamma(\omega) = (1/4\pi\epsilon_0)(4\omega^3 |\vec{d}|^2 / 3\hbar c^3)$. Considering a two-level system, we write the unperturbed Hamiltonian as $H_S = (\hbar\omega_0/2)(|2\rangle\langle 2| - |1\rangle\langle 1|) = (\hbar\omega_0/2)\sigma_z$ and $H_I = \vec{D}\vec{E}$ as the interaction with the fluctuating field operator. In an N-level system there are at most N^2 independent Lindblad operators. Here, we discuss two cases. When the environment couples level $|1\rangle$ to level $|2\rangle$ only, i.e., $\vec{D} = \vec{d}|1\rangle\langle 2|$, one obtains

$$L(\omega_0) = \sqrt{\gamma_0}|1\rangle\langle 2| = \sqrt{\gamma_0}\sigma_+,$$

$$L^\dagger(\omega_0) = \sqrt{\gamma_0}|2\rangle\langle 1| = \sqrt{\gamma_0}\sigma_-, \qquad (23)$$

with $\gamma_0 = (1/4\pi\epsilon_0)(4\omega_0^3 |\vec{d}|^2 / 3\hbar c^3)$. $\sigma_- = 1/2(\sigma_x - i\sigma_y)$, $\sigma_+ = 1/2(\sigma_x + i\sigma_y)$, where σ_x, σ_y, and σ_z are the Pauli matrices. Neglecting the Lamb shift, we can now write the dissipative superoperator in the form

$$L_D[\rho(t)] = \frac{\gamma_0}{2} \left(\sigma_+ \rho(t) \sigma_- - \frac{1}{2}\{\sigma_+\sigma_-, \rho(t)\} \right). \qquad (24)$$

The contribution to the evolution of the density-atrix elements from the environment (E) is thus

$$\partial_t \rho_{11E} = \gamma_0 \rho_{22}, \qquad (25)$$

$$\partial_t \rho_{12E} = -\frac{\gamma_0}{2} \rho_{12}, \qquad (26)$$

$$\partial_t \rho_{22E} = -\gamma_0 \rho_{22}. \tag{27}$$

We observe that the population decays exponentially with rate $\gamma_0 = 1/T_1$, while coherence decays with $\gamma_0/2 = 1/T_2 = 1/2T_1$. The population relaxation (T_1 process) induces also the destruction of coherence (T_2 process). Now, if the environmental coupling is diagonal in ground and excited state, we have

$$\vec{D} = \vec{d}_g|1\rangle\langle 1| + \vec{d}_e|2\rangle\langle 2| = \vec{d}_g \mathcal{I} + (\vec{d}_e - \vec{d}_g)|2\rangle\langle 2|, \tag{28}$$

where we have used the closure relation $\mathcal{I} = |1\rangle\langle 1| + |2\rangle\langle 2|$. The unity operator $\mathcal{I}$ commutes with the system Hamiltonian and cannot cause any relaxation. Thus the Lindblad operator takes the form

$$L(\omega_0) = \sqrt{\gamma_0}|2\rangle\langle 2| = \sqrt{\gamma_0}\frac{(\mathcal{I} + \sigma_z)}{2},$$

$$L^\dagger(\omega_0) = L(\omega_0), \tag{29}$$

with $\gamma_0 = (1/4\pi\epsilon_0)[4\omega_0^3|(\vec{d}_e - \vec{d}_g)|^2/3\hbar c^3]$ and leads to

$$L_D[\rho(t)] = \gamma_0 \left(\frac{\mathcal{I} + \sigma_z}{2}\rho(t)\frac{\mathcal{I} + \sigma_z}{2} - \frac{1}{2}\left\{ \frac{\mathcal{I} + \sigma_z}{2}, \rho(t) \right\} \right). \tag{30}$$

The environmental contribution to the evolution of the system is thus

$$\partial_t \rho_{11E} = 0, \tag{31}$$

$$\partial_t \rho_{12E} = -\frac{\gamma_0}{2}\rho_{12}, \tag{32}$$

$$\partial_t \rho_{22E} = 0. \tag{33}$$

In this case, there is pure-T_2 dephasing involving only the destruction of coherence ρ_{12} but there is no direct effect on population ρ_{11} and ρ_{22}.

In atomic systems, the magnitude of typical wave vectors, $k = \omega/c$, is of the order of 10^{-5} cm^{-1} (optical domain). If we approximate the dipole moment by Bohr's radius, $|\vec{d}| \simeq a_B$, the lifetime $\tau = 1/\gamma$ is roughly 10^{-8} s which is much larger than the typical period of oscillation $\mathcal{T} = (c|k|)^{-1} = 10^{-15}$ s. Atoms decay rather slowly and the energy levels are relatively stable. In case of atomic transitions, the interaction of the physical system with the environment (vacuum fluctuations) should be controllable. Contrary to atoms, solids are characterized by very short electron-hole dephasing times due to carrier-carrier and carrier-phonon scattering, sometimes as low as a few tens of femtoseconds [26–28]. On this time scale, the interplay between coherent and incoherent dynamics is very strong. Consequently, coherent control of the electron dynamics in these systems is a difficult task and optimization of the control fields is essential.

V. NUMERICAL RESULTS

We demonstrate the effectiveness of our optimum control schemes at several examples of dissipative *N*-level systems. We consider the following model for the driven *N*-level system. The free evolution of *N*-level system is governed by the internal Hamiltonian whose form is

$$H_0 = \sum_{n=1}^{N} E_n |n\rangle\langle n|. \tag{34}$$

We choose the level sequence to be

$$E_{n+1} = E_n + \frac{\Delta E}{n}, \quad n = 1, 2, 3, \ldots.$$

The ground state $E_1 = 0$ and $\Delta E = \pi e V$. The interaction of the system with the control field, in the dipole approximation, is chosen to be

$$H_I = \sum_{n,m=1}^{N} D_{nm} E(t) |n\rangle\langle m| = d\, E(t) \sum_{n=1}^{N-1} (|n\rangle\langle n+1| + |n+1\rangle\langle n|)$$
$$= \hbar \varepsilon(t) \sum_{n=1}^{N-1} (|n\rangle\langle n+1| + |n+1\rangle\langle n|), \tag{35}$$

where d is the dipole matrix element between the levels n and $n+1$ and $\varepsilon(t) = dE(t)/\hbar$.

We consider a situation in which the electric field is small (zero) at the initial time, as will usually be the case in experiment. As discussed in Sec. II this is enforced by the time-dependent weight factor $\alpha(t)$ in the cost functional Eq. (3). Specifically, it is given by the form

$$\alpha(t) = \alpha_0 + W_0 \exp(-t/n) + W_T \exp[-(M - t)/n], \tag{36}$$

where M is the number of mesh point (the dimension of the optimal problem). In our numerical simulation we take $\alpha_0 = 10^{-3}$, $W_0 = 10^2$, and $n = 50$. In the dissipation-free case $W_T = 10^2$, else it is set equal to zero.

In all cases discussed below, the initial guess for an optimum electric field for the dissipation-free case is a weak random field with constant distribution between zero and one. When we increase dissipation in the system step by step, we use the final optimal solution from the previous case for the initial guess.

The interaction of the physical system with its environment is represented by the Lindblad operators, as detailed in the previous section at the example of the two-level system. In all examples below, we consider the Lindblad operators to be of the form

$$L_\mu = \sqrt{\gamma}|n_\mu\rangle\langle m_\mu|, \tag{37}$$

that is, proportional to one and the same factor $\sqrt{\gamma}$, where $\gamma = 1/\tau_D$ and $\tau_D = 10^n T$, with $n = 1, 0, -1, -2$.

For example, considering the Lindblad operators

$$L_\mu = \sqrt{\gamma}|n_\mu\rangle\langle m_\mu|, \tag{38}$$

for $n_\mu < m_\mu$, with $n_\mu = 1, \ldots N-1$, and $m_\mu = 2, \ldots N$, one obtains for the environmental contribution

$$\dot{\rho}_{\alpha\alpha E} = \gamma \sum_{l=\alpha+1}^{N} \rho_{ll} - \gamma(\alpha - 1)\rho_{\alpha\alpha}, \quad \text{for } \alpha = 1, \ldots N \tag{39}$$

and

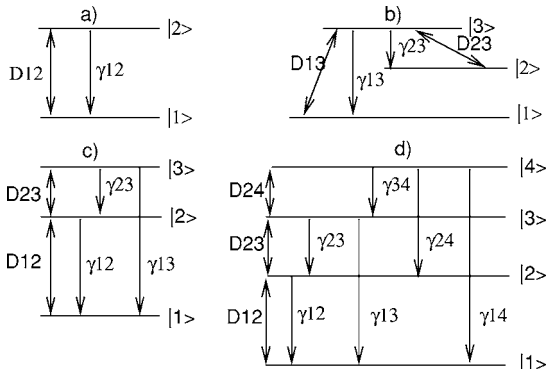

FIG. 1. Various configurations used in our simulation: two-level system (a), three-level-Λ system (b), three-level-ladder system, (c) and four-level-ladder system (d).

$$\dot{\rho}_{\alpha\beta E} = -\frac{\gamma}{2}(\alpha+\beta-2)\rho_{\alpha\beta}, \quad \text{for } \alpha \neq \beta = 1,\ldots N. \quad (40)$$

In this paper we consider the time evolution of dissipative two-, three-, and four-level systems. We study a time evolution which takes the system from its ground state at time zero into a specified final state at target time T. In all cases the target time T is chosen to be 50 fs and the time step is 10^{-2} fs. For the three- and four-level Λ configuration the target state is the second energy level. In all other cases, the target state is the uppermost energy level. The various situations are sketched in Fig. 1. Our aim is to find a control field that achieves perfect population transfer by solving the optimal control problem with the indirect method outlined above.

A. Two-level system

We first consider the case without dissipation. From analytic solutions within the rotating-wave approximation we know that there are many solutions to this problem, such as a series of solutions with constant field amplitudes and a frequency which is resonant to the transition. In this particular calculation, we suppress the electric field at initial and target time via the weight factor $\alpha(t)$ in Eq. (36) to limit the number of solutions and provide a framework which is more realistic with respect to experiment. Furthermore, we strive for weak electric fields in the initial guess and by our choice for $\alpha(t)$ favor weak electric fields for our optimum fields. Without dissipation, this objective was met perfectly by our approach. Within half a "Rabi oscillation" the population is transferred from ground to excited state in the most economical way. As expected, the optimal electric field peaks near the fundamental frequency of the two-level system. Note, however, that here the transfer is achieved by a pulsed electric field, rather than a plane-wave electric field.

For the dissipative two-level system, we consider two distinctly different cases: (i) pure dephasing and (ii) population decay, which is inevitably associated with dephasing. The first case is achieved by a Lindblad operator which is diagonal in the two-level basis states, Eq. (29), such as

$$L = \sqrt{\gamma}|1\rangle\langle 1| = \begin{pmatrix} \sqrt{\gamma} & 0 \\ 0 & 0 \end{pmatrix}. \quad (41)$$

For the second case, we choose the Lindblad operator

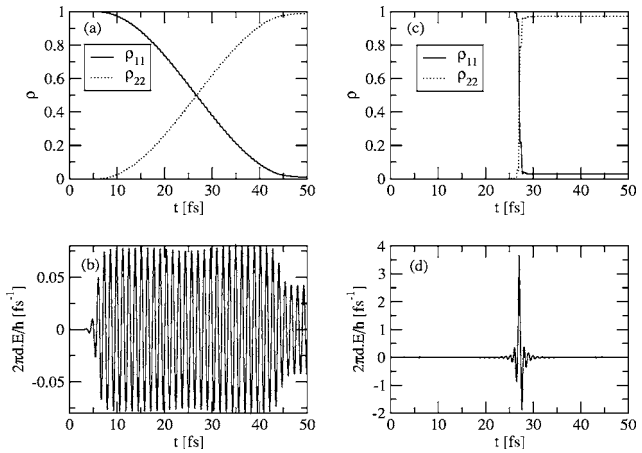

FIG. 2. Dissipative two-level system (pure dephasing effect): (a) and (b), respectively, show the population transfer from the ground state $|1\rangle$ to the stable excited state $|2\rangle$ and the optimal control field for $\tau_D = 10T$ (weak damping regime). (c) and (d), respectively, show the population transfer from the ground state $|1\rangle$ to the stable excited state $|2\rangle$ and the optimal control field for $\tau_D = 10^{-1}T$ (strong damping regime). $E_2 - E_1 = 3.14$ eV, $\omega = 4.7 \times 10^3$ THz, oscillation period $\mathcal{T} = 1.31$ fs, target time $T = 50$ fs, and time step 10^{-2} fs.

$$L = \sqrt{\gamma}|1\rangle\langle 2| = \begin{pmatrix} 0 & \sqrt{\gamma} \\ 0 & 0 \end{pmatrix}. \quad (42)$$

In case of pure dephasing, Fig. 2 shows the energy level population versus time for the optimum control field and increasing dephasing rate, as obtained by the gradient method. According Figs. 2(a) and 2(b) one finds that, as long as the coherence time is larger than the target time T, almost perfect transfer into the upper level is achieved. As the coherence time decreases, population transfer becomes less complete and occurs at an increasingly higher rate as shown in Figs. 2(c) and 2(d). This is facilitated by pulses of decreasing duration and increasing amplitude. We have also computed the power spectrum of the electric field. We find that the spectral width of the electric field increases around the two-level resonance with the decay rate of polarization. The physical explanation is as follows. For the present model of dissipation and in the absence of the external electric field, the target state is a stable state. Once the transfer has been accomplished it will be maintained indefinitely. When the coupling to the reservoir is increased the decay rate of the interband polarization increases accordingly and a short strong electric pulse which leads to a polarization which is also peaked in time is more efficient in achieving the task, since there is less time for unwanted polarization decay. Once the transfer has been achieved as completely as possible, decay of interband polarization is of no further concern. The present numerical results for the final population of the upper level can be improved by reducing the value for α_o in Eq. (36), which is a measure for the relative importance of reaching the target state and keeping electric fields at moderate values. In this sense, pure dephasing places a relatively simple problem to achieving optimum control. Remarkably, near perfect transfer can be achieved even when τ_D is less than the intrinsic oscillation period $\mathcal{T}$ of the two-level sys-

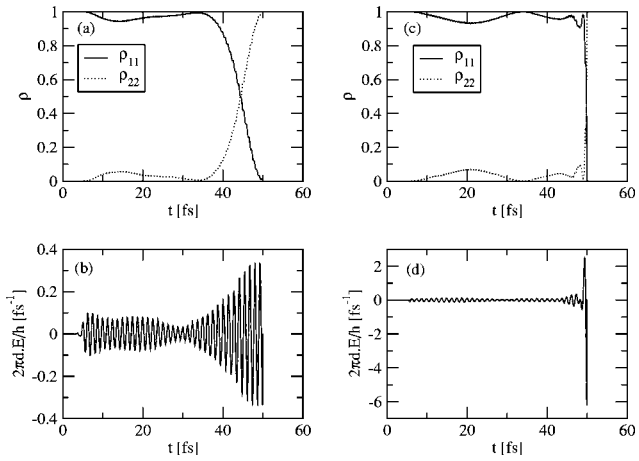

FIG. 3. Dissipative two-level system (relaxation effect): (a) and (b), respectively, show the population transfer from the ground state $|1\rangle$ to the unstable excited state $|2\rangle$ and the optimal control field for $\tau_D=10T$ (weak damping regime). (c) and (d), respectively, show the population transfer from the ground state $|1\rangle$ to the unstable excited state $|2\rangle$ and the optimal control field for $\tau_D=10^{-1}T$ (strong damping regime). $E_2-E_1=3.14$ eV, $\omega=4.7\times10^3$ THz, oscillation period $\mathcal{T}=1.31$ fs, target time $T=50$ fs, and time step 10^{-2} fs.

tem. When $\tau_D<\mathcal{T}$ the system tends to seek a state of equal population of the two levels for less than optimal electric fields. Figure 2(d) shows that if one can generate electric-field pulses shorter than the τ_D and of sufficient strength, the desired population can be achieved to a high degree. This is in agreement with the so-called "bang-bang?" method where one seeks pulse durations shorter than the shortest characteristic dephasing time [29–32].

The second case considers the situation of both polarization and population decay. Now the target state of the dissipative two-level system is no longer stable and early population of the target state is undesirable. In these simulations we do not suppress the electric field near target time T via $\alpha(t)$. Figure 3 displays our results for this situation. Again, increasing the coupling to the environment and thus making τ_D shorter increases the electric field and decreases its duration. In addition, the "time of arrival" of the main field contribution is shifted closer and closer to target time T. The reason is that the instability of the final state and the requirement of small electric fields make it favorable that it be populated only just at target time to avoid premature decay. Even in case of strong dissipation ($\tau_D=10^{-1}\ T$) one achieves good control, provided that sufficiently strong and short pulses can be generated. As will be discussed later, based on the present model for dissipation, the electric field cannot stabilize the target state from decay and this "last-minute" driving represents the only option within the present model.

B. Three-level system

The three-level system offers a much higher parameter space and richness in physics than the two-level system. We apply the simplifications as outlined in the introduction above. Electromagnetically driven three-level systems have been widely studied in the literature, both theoretically and experimentally. They offer a basic understanding of stimulated Raman adiabatic passage (STIRAP) and related phenomena, such as electromagnetically induced transparency, slowing of light, optical gain without inversion, and state trapping [33,34].

We first consider the elementary Λ configuration as sketched in Fig. 1(b). The three-level system has a stable ground state $|1\rangle$ and a stable target state $|2\rangle$ between which direct dipole transitions are forbidden. There is dipole coupling between $|1\rangle$ and $|3\rangle$, as well as $|2\rangle$ and $|3\rangle$. The uppermost level $|3\rangle$ is unstable with respect to decay into levels $|1\rangle$ and $|2\rangle$, which is represented by the Lindblad operators from $|3\rangle$ to $|1\rangle$.

For the dissipation-free case which was studied with the conjugate gradient method and a random initial electric-field "perfect" transfer can be achieved. This is to be expected since we are in the adiabatic regime. Inspection of the selected optimal electric field, however, shows a small surprise. While the spectral composition corresponds to the two resonant dipole transitions, the algorithm did not select the "counterintuitive" STIRAP sequence of pulses, first the low-frequency pulse which couples levels 2 and 3 and then the high-frequency pulse coupling 1 to 3. Rather, it selected an "intuitive" sequence where one has the high-frequency pulse first and then the low-frequency contribution at the tail end (right end) of the pulse. The chosen pulse scheme leads to significant population of level 3 (about 0.4), which in this case has not been discouraged or suppressed since this level is stable. Frequency contributions peak at $\omega_{32}=2.38\times10^3$ THz and $\omega_{31}=7.15\times10^3$THz, corresponding to the dipole-allowed transitions. Moreover, there is level-1-2 polarization which is comparable in size to the other interlevel polarizations which correspond to dipole-allowed transitions.

The situation changes, when level 3 is made unstable by increasing the coupling strength γ from value zero. This is shown in Fig. 4. With decreasing τ_D, population of level 3 becomes less and less desirable and the electric field is forced to follow the STIRAP scheme, with the high-frequency contribution trailing the low-frequency contribution, as seen in Fig. 4(d). As for the two-level system, a decrease of τ_D goes hand in hand with an increase in electric field and the width of the peaks, however, not as dramatic as in the two-level case. A third small peak at high frequency centered at about $2\omega_{31}-\omega_{32}$ emerges at the expense of the peak near ω_{32}. While polarizations ρ_{13} and ρ_{12} perform simple driven harmonic Rabi-type oscillations, ρ_{23} is found to undergo anharmonic (multifrequency) oscillations, with frequency contributions from ω_{32}, ω_{31}, and $2\omega_{31}-\omega_{32}$. We interpret this as the emergence of a two-photon process which avoids level 3. Photons of frequency $2\omega_{31}-\omega_{32}$ get absorbed in conjunction with the emission of a photon of frequency ω_{31}. This allows a direct population transfer from level 1 to level 2, by passing the unstable level 3.

Figure 5 shows an open three-level Λ system where 3 is unstable to decay into a fourth level which does not couple to the electromagnetic field. The dash-dotted line shows the population of level 4 (probability of escaping the system). Control in this system is more demanding since particles lost from the three-level system cannot be recovered and there is "nonfriendly" decay which helps to transfer particles from

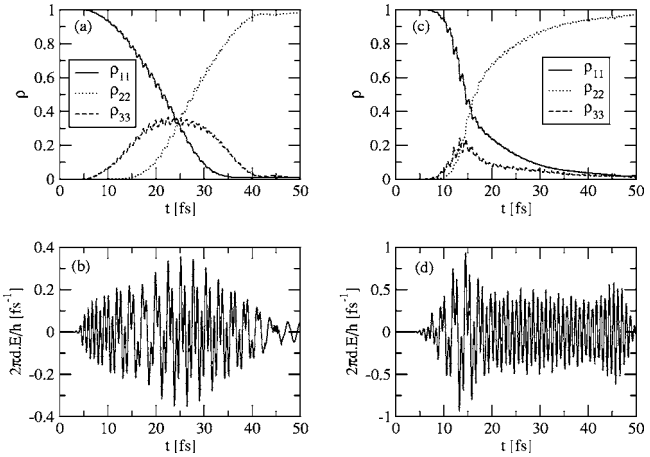

FIG. 4. Dissipative three-level-Λ system (population decay from $|3\rangle$ to $|1\rangle$ and from $|3\rangle$ to $|2\rangle$): (a) and (b), respectively, show the population transfer from the ground state $|1\rangle$ to the stable state $|2\rangle$ and the optimal control field for $\tau_D=10T$ (weak damping regime). (c) and (d), respectively, show the population transfer from the ground state $|1\rangle$ to the stable state $|2\rangle$ for $\tau_D=10^{-1}T$ (strong damping regime). $E_3-E_1=4.71$ eV, $E_3-E_2=1.57$ eV, $\omega_{31}=7.15\times10^3$ THz, $\omega_{32}=2.38\times10^3$ THz, oscillation periods $\mathcal{T}_{31}=0.87$ fs, $\mathcal{T}_{32}=2.63$ fs, target time $T=50$ fs, and time step 10^{-2} fs.

level 3 into target state level 2. This is evident from a comparison of Figs. 4 and Fig 5.

We now return to the discussion of the ladder-type configuration, now consisting of three levels. Starting with the dissipation-free situation, the optimum field selected by starting from a random field is one which, essentially, first pumps particles from level 1 into level 2 and subsequently from level 2 into level 3. Complete transfer into level 3 is achieved.

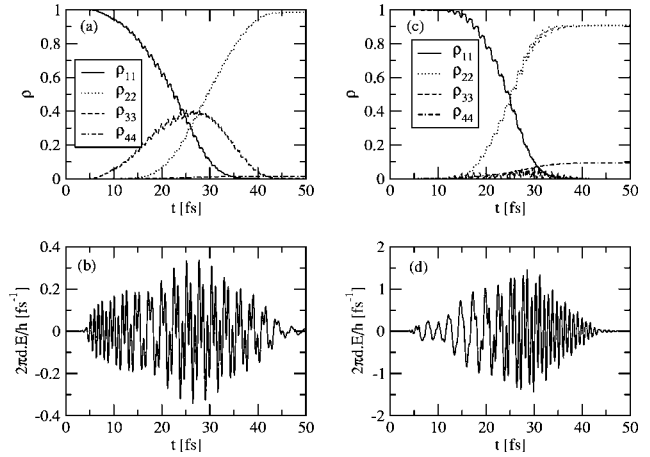

FIG. 5. Dissipative three-level-Λ system (population decay from $|3\rangle$ to auxiliary state $|4\rangle$): (a) and (b), respectively, show the population transfer from the ground state $|1\rangle$ to the stable state $|2\rangle$ and the optimal control field for $\tau_D=10T$ (weak damping regime). (c) and (d), respectively, show the population transfer from the ground state $|1\rangle$ to the stable state $|2\rangle$ for $\tau_D=10^{-1}T$ (strong damping regime). $E_3-E_1=4.71$ eV, $E_3-E_2=1.57$ eV, $\omega_{31}=7.15\times10^3$ THz, $\omega_{32}=2.38\times10^3$ THz, oscillation periods $\mathcal{T}_{31}=0.87$ fs, $\mathcal{T}_{32}=2.63$ fs, target time $T=50$ fs, and time step 10^{-2} fs.

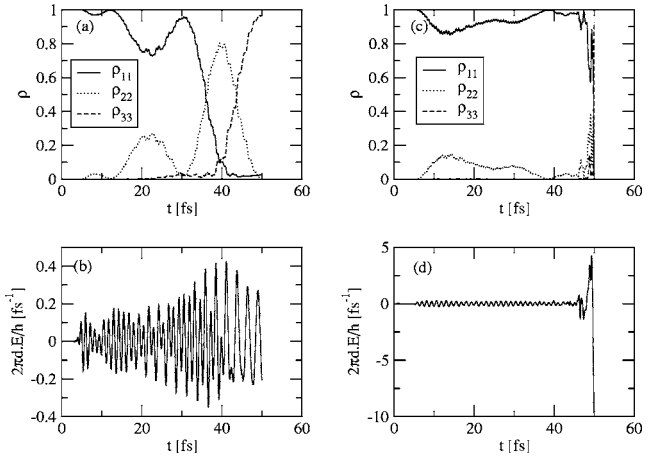

FIG. 6. Dissipative three-ladder system: (a) and (b), respectively, show the population transfer from the ground state $|1\rangle$ to the unstable excited state $|3\rangle$ and the optimal control field for $\tau_D=10T$ (weak damping regime). (c) and (d), respectively, show the population transfer from the ground state $|1\rangle$ to the unstable excited state $|3\rangle$ and the optimal control field for $\tau_D=10^{-1}T$ (strong damping regime). $E_3-E_2=1.57$ eV, $E_2-E_1=3.14$ eV, $\omega_{32}=2.38\times10^3$ THz, $\omega_{21}=4.7\times10^3$ THz, oscillation periods $\mathcal{T}_{32}=2.63$ fs, $\mathcal{T}_{21}=1.31$ fs, target time $T=50$ fs, and time step 10^{-2} fs.

In order to study a dissipative three-level ladder system, we use the Lindblad operators

$$L_1=\sqrt{\gamma}|1\rangle\langle2|,\quad L_2=\sqrt{\gamma}|1\rangle\langle3|,\quad L_3=\sqrt{\gamma}|2\rangle\langle3| \tag{43}$$

to incorporate coupling to the environment. Now both levels 2 and 3 are unstable, with levels 2 and 3, respectively, having a lifetime of τ_D and $\tau_D/2$. Again, we successively increase the coupling and use the optimum solution from the previous case as the starting point for the next case. The results are summarized in Fig. 6. Since the goal is to arrive at maximum population at target time $T=50$ fs, the action of the electric field is successively delayed with increasing γ. However, comparing with the dissipation-free case, the population dynamics changes its nature. The intermediate level gets populated and depopulated several times, however, only to a smaller and smaller degree. The system is preconditioned for the big boost in the electric field which eventually drives the population into the target state. As γ increases the frequency spectrum of the electric field rapidly gains complexity. Up to $\tau_D\approx T$, the two frequency peaks corresponding to the dipole-allowed transitions dominate, then higher frequency components gain equal weight. The success rate of at least 90% up to $\tau_D\approx10^{-2}\ T$ is quite remarkable. It is also remarkable that for the three-level system the electric-field strength increase is less dramatic as in the two-level case, but the frequency spectrum becomes less peaked. In the two-level case, it is essentially field strength and pulse duration which is used to achieve the task. In the three-level case, it is to a large extent the increase in frequency contributions to the electric field which compensates for increased dissipation.

C. Four-level system

We also explored open and closed four-level Λ schemes consisting of a stable ground state $|1\rangle$ and a stable target state

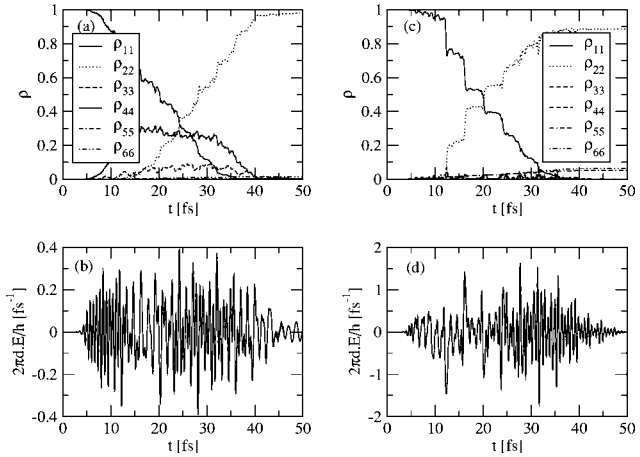

FIG. 7. Dissipative four-level Λ system (population decay from $|3\rangle$ to auxiliary state $|5\rangle$ and population decay from $|4\rangle$ to auxiliary state $|6\rangle$): (a) and (b), respectively, show the population transfer from the ground state $|1\rangle$ to the stable excited state $|2\rangle$ and the optimal control field for $\tau_D=10T$ (weak damping regime). (c) and (d), respectively, show the population transfer from the ground state $|1\rangle$ to the stable excited state $|2\rangle$ and the optimal control field for $\tau_D=10^{-1}T$ (strong damping regime). $E_4-E_1=1.04$ eV, $E_3-E_2=1.57$ eV, $E_2-E_1=3.14$ eV, $\omega_{43}=1.59\times10^3$ THz, $\omega_{32}=2.38\times10^3$ THz, $\omega_{21}=4.77\times10^3$ THz, oscillation periods $\mathcal{T}_{43}=3.94$ fs, $\mathcal{T}_{32}=2.63$ fs, $\mathcal{T}_{21}=1.31$ fs, target time $T=50$ fs, and time step 10^{-2} fs.

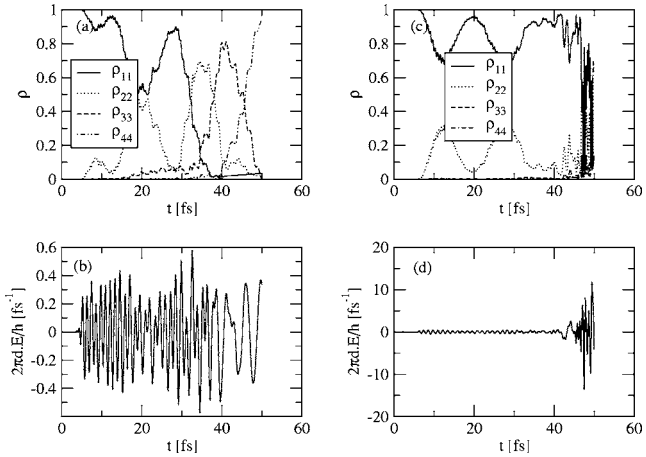

FIG. 8. Dissipative four-level-ladder system: (a) and (b), respectively, show the population transfer from the ground state $|1\rangle$ to the unstable excited state $|4\rangle$ and the optimal control field for $\tau_D=10T$ (weak damping regime). (c) and (d), respectively, show the population transfer from the ground state $|1\rangle$ to the unstable excited state $|4\rangle$ and the optimal control field for $\tau_D=10^{-1}T$ (strong damping regime). $E_4-E_1=1.04$ eV, $E_3-E_2=1.57$ eV, $E_2-E_1=3.14$ eV, $\omega_{43}=1.59\times10^3$ THz, $\omega_{32}=2.38\times10^3$ THz, $\omega_{21}=4.77\times10^3$ THz, oscillation periods $\mathcal{T}_{43}=3.94$ fs, $\mathcal{T}_{32}=2.63$ fs, $\mathcal{T}_{21}=1.31$ fs, target time $T=50$ fs, and time step 10^{-2} fs.

$|2\rangle$ between which direct dipole transitions are forbidden. Considering an open four-level scheme, there are two intermediate states $|3\rangle$ and $|4\rangle$, from which there is decay to levels outside of the system introduced by Lindblad operators

$$L_1=\sqrt{\gamma}|5\rangle\langle 3|, \quad L_2=\sqrt{\gamma}|6\rangle\langle 4|, \tag{44}$$

where $|5\rangle$ and $|6\rangle$ denote states outside the four-level system which serve as a sink for the particle. In this case, once the particle is lost from the system, it cannot be "recycled" by the electric field. There is dipole coupling between levels $|1\rangle$ and $|3\rangle, |1\rangle$ and $|4\rangle$, as well as $|2\rangle$ and $|3\rangle$, and $|2\rangle$ and $|4\rangle$. Levels 5 and 6 do not interact with the electric field.

In the dissipationless case, we again obtain the "intuitive" solution transferring the particle via levels 3 and 4. Results for the dissipative case with $\gamma=1/T$ and $\gamma=10/T$ are shown in Fig. 7. Again, transfer can be achieved to a high degree. In the strong damping regime a transfer occurs in bursts (a steplike fashion). Now dissipation enforces the "counterintuitive" pulse sequence. Note, however, that in contrast to analytical studies, here we do not rely on the rotating-wave approximation nor do we distinguish between different field components which are coupled solely to a particular transition [15].

Finally, we discuss results obtained for the ladder-type four-level system. For the dissipationless case we find the step-by-step transfer of population which was seen already for the three-level system. Hence the optimum electric field starts with high-frequency contributions and ends with low-frequency contributions, as seen in Fig. 8. Moreover, the goal of complete population of the fourth level was accomplished by a pulsed field which is zero at $t=0$ and at target time TIt should be noted that the average field intensity is higher than in case of two- and three-level systems. The reason is that intermediate levels 2 and 3 need to be populated within a fraction of the target time T.

The dissipative four-level system was investigated for the Lindblad operators

$$L_1=\sqrt{\gamma}|1\rangle\langle 2|, \quad L_2=\sqrt{\gamma}|1\rangle\langle 3|, \tag{45}$$

$$L_3=\sqrt{\gamma}|1\rangle\langle 4|, \quad L_4=\sqrt{\gamma}|2\rangle\langle 3|, \tag{46}$$

$$L_5=\sqrt{\gamma}|2\rangle\langle 4|, \quad L_6=\sqrt{\gamma}|3\rangle\langle 4|. \tag{47}$$

The corresponding lifetimes of levels 2, 3, and 4, respectively, are $\tau_D, \tau_D/2$, and $\tau_D/3$. Polarization ρ_{12}, ρ_{13}, and ρ_{23} decay with a lifetime $\tau_D/2, \tau_D$, and $3/2\tau_D$, respectively. With increasing dissipation, it becomes less favorable to do the simple sequential transfer from level to level. Rather, and as already observed for the dissipative three-level ladder system, several cycles of pumping between ground state and intermediate levels are performed. It should be kept in mind that population lost in upper levels shows up in lower levels. Finally, population is transferred from level 3 and, to a lesser extent, from level 2 into the target state level 4. In this relatively complicated system, the success rate is more sensitive to dissipation. Nevertheless, for $\tau_D=10T$, $\tau_D=T$, $\tau_D=10^{-1}T$, and $\tau_D=10^{-2}T$, respectively, we still obtain success rates of about 90%, 80%, 70%, and 60%. In case that a direct dipole transition between level $|1\rangle$ and $|4\rangle$ is allowed, the optimal field selects essentially this direct transition.

The main difference between the STIRAP and the ladder systems considered here is that for the former the target state

is stable with respect to decay. Due to the present model for dissipation, in form of Lindblad operators with constant decay rates, the electric field can do nothing to stabilize the target state. In particular, an electric field could not trap the system in an instable target state. This can be seen using the concept of purity in conjunction with the present dynamic equation. One may define purity P, $0 \leqslant P \leqslant 1$, as

$$P = 2\mathrm{Tr}\{\rho^2\} - \mathrm{Tr}\{\rho\}. \tag{48}$$

The rate of change of P is given by

$$\dot{P}(t) = \sum_{\mu} \mathrm{Tr}\{\rho(t) L_\mu \rho(t) L_\mu^\dagger - \rho(t) L_\mu^\dagger L_\mu \rho(t)\}. \tag{49}$$

Due to the cyclicity of the trace, the unitary contribution to the time evolution containing the control field does not enter. The electric field merely influences the evolution of $\rho(t)$. Within the present model for the Lindblad operators in Eq. (38),

$$\dot{P}(t) = \sum_{\mu} \gamma_\mu [\rho_{i_\mu i_\mu} \rho_{j_\mu j_\mu} - (\rho^2)_{j_\mu j_\mu}]. \tag{50}$$

For a pure state to be stationary with respect to decay channel μ, the state needs to fulfill $(\rho_{i_\mu i_\mu} - 1)\rho_{j_\mu j_\mu} = 0$.

Consider, for example the two-level system and the density operator

$$\rho = \frac{1}{2}(1 + \boldsymbol{\sigma} \cdot \mathbf{p}), \quad 0 \leqslant p^2 \leqslant 1, \tag{51}$$

where $\boldsymbol{\sigma}$ is the Pauli vector and purity $P = p^2$. For the Lindblad operator $Ł = \sqrt{\gamma}|1\rangle\langle 2|$, the stationarity condition is $p^2 + p_z^2 - 2p_z = 0$ and the only stable pure state is the ground state $|1\rangle$. A stationary mixed state is $p_x = p_x = p_x = 1/2$, with purity $P = \frac{3}{4}$. For the "pure-dephasing" Lindblad operator $Ł = \sqrt{\gamma}|2\rangle\langle 2|$, the stationarity condition is $p^2 = p_z^2$. Hence $p_x = p_y = 0$ and $p_z = \pm 1$, corresponding to levels $|1\rangle$ and $|2\rangle$, respectively, are the only stable states.

VI. SUMMARY AND CONCLUSIONS

In summary, we have formulated a general class of optimization problems where the constraint is a dynamical evolution of the system under the Lindblad equation within Pontriyagin's minimum principle. This formulation of problem leads to an indirect method equivalent to the Lagrangian multiplier method which leads to the an introduction of an adjoint field (co-state) for which the time evolution needs to be solved backwards in time. The kinetic equations and the initial conditions at target time T for the co-state depend, next to the kinetic equations for the density operator, on the cost functional. The co-state enters the expressions for the optimum field solution and the gradient of the cost functional.

For the numerical part, we have adapted the conjugate gradient method to study optimum coherent control in dissipative N-level systems. In the present study, the problem posed was to transfer population from the (nondegenerate) ground state of the system in which it resides at $t = 0$ to a target state at specified time T, using weak electric fields whenever possible. We concentrated on a ladder-type N-level system for which an electric field can induce dipole transitions between adjacent energy levels and Λ schemes, as used in STIRAP experiments. For the former, the ground state of the system was chosen to be stable and excited states were chosen unstable to account for interaction with the "environment" whose action was characterized by Lindblad operators. For simplicity of presentation of results, we considered only cases where the coupling strength is the same for all Lindblad operators. The main difference to the Λ scheme is that for the latter the target state was assumed to be stable (on the time scale of the simulation).

Our studies demonstrate that the conjugate gradient method is a powerful tool for optimum control in quantum systems. Even when starting from random fields which do not account for the intrinsic structure of the quantum system, we have been able to reach convergence, albeit, after as many as 500 iterations. "Educated guesses" when going from one optimum solution to the case of stronger dissipation or starting from optimal solution from direct methods using a small parameter set lead to convergence within typically 100 iterations.

For the dissipation-free case we find that perfect transfer can be achieved most economically by a successive level-to-level transfer. Our calculations for up to $N = 8$, not shown here for brevity, confirm this scenario also for more complicated systems. For the dissipation-free case, we were able to present suggestions for optimal control based on electric fields whose amplitude goes to zero smoothly at the boundaries of the time interval, as one would wish in experiment. In the dissipation-free Λ scheme, the optimum solution selected by this indirect method was inevitably the intuitive pulse sequence following the dipole-allowed transitions and not the STIRAP sequence. The reason is that our cost functional penalizes field intensity. It is less intensity-effective to establish the adiabaticity condition for a given time interval T via intensity than to resonantly transfer the particle via the intermediate levels.

For all systems studied, i.e., two-, three-, and four-level systems, we find that the weak-dissipation limit as it is relevant for atomic and many molecular systems, poses no serious threat to success. Electric fields tend to be larger than for the dissipation-free case and their onset is delayed closer and closer to target time. As the complexity of a system, such as the number of (unstable) levels and decay channels, increases the degree of success decreases, as expected. However, even for rather unrealistic decay times which are shorter than the characteristic periods of the N-level system, optimum control has success rates well in excess of 50%, making, for example, majority voting a meaningful error correction scheme. These ultrashort lifetimes were chosen not so much for physical reasons, but to test the prowess of the numerical approach. Nevertheless, our results give encouragement that in realistic systems which are characterized by short decoherence times, such as semiconductor-based mesoscopic structures, coherent steering of the system's dynamics should be accomplishable with high fidelity.

Since the target state was, in general, not a stable state, electric fields at target time were not equal to zero. More-

over, had the field been turned off, the target state would have decayed according to its lifetime. An interesting question is to what extent an external (electric) field can stabilize a system in a prescribed quantum state in the presence of dissipation, in other words, to what extent an electric field can trap a quantum system in an otherwise unstable state. Inspection of the Lindblad equation with fixed decay rates γ shows that the electric field cannot control the decay of purity. Due to the cyclicity of the trace, the unitary contribution to the time evolution, to which the electric field contributes, does not contribute to decay of purity. Hence within the present model of decay, the electric field is not able to counteract the decay of the target state. This is the reason why, for the ladder system in the high dissipation regime, the optimal field is the one which accomplishes the transfer "in the last minute." In the Λ scheme the situation is different in the ladder scheme in that the target state is stable. This eases the optimization problem and allows electric fields of longer pulse duration as compared to the ladder system, where the field has to cope with decay of the target state.

One of the drawbacks of the present numerical approach is that the iteration loop contains a backwards integration in time for the adjoined state. For linear systems, this equation is similar in its structure to the forward-in-time equation for the physical state of the system. In nonlinear systems, such as relevant in the description of interacting many-body systems, the backwards-equation in time may be considerably different from the forward equation and its derivation and execution cumbersome. Therefore we have also developed direct methods which rely on some physical intuition and use a small number of parameters. We found that direct parametrization can be very successful. A comparison to the indirect method used here and application to interacting many-body systems will be given elsewhere.

ACKNOWLEDGMENT

We wish to acknowledge financial support of this work by FWF, Project No. P16317-N08.

APPENDIX: EXPLICIT DERIVATION OF THE STATIONARITY CONDITIONS

The stationarity conditions (6) are derived by computing the variation of the augmented cost functional,

$$\bar{J} := \mathrm{Tr}\{\Phi_o(\rho(T))\} + \int_0^T \{\mathcal{H}(\rho(t),\varepsilon(t),\lambda(t)) - \mathrm{Tr}[\lambda(t)\rho_t(t)]\}dt. \tag{A1}$$

The integrant in the second term of $\bar{J}$ is the Legendre transformed of the canonical Hamiltonian $\mathcal{H}$ [35–37]. We use with $(\cdot)_t \equiv (d/dt)(\cdot)$. The minimization of $\bar{J}$ leads to a link between the objective functional J and the optimal solution $\varepsilon(t)$ supplied by the Lagrange multiplier matrix. Integration by parts of the last term on the right side of Eq. (A1) yields

$$\bar{J} := \mathrm{Tr}\{\Phi_o(\rho(T))\} - \mathrm{Tr}\{\lambda(T)\rho(T)\} + \mathrm{Tr}\{\lambda(0)\rho(0)\} + \int_0^T [\mathcal{H}(\rho(t),\varepsilon(t),\lambda(t)) + \mathrm{Tr}\{\lambda_t(t)\rho(t)\}]dt. \tag{A2}$$

Now consider the variation in $\bar{J}$ due to the variations in the control field $\varepsilon(t)$ and $\rho(T)$ [keeping $\lambda(t)$ constant]

$$\delta\bar{J} := \mathrm{Tr}\{[\Phi'_o(\rho(T)) - \lambda(T)]\delta\rho(T)\} + \int_0^T \mathrm{Tr}\left\{\left(\frac{\partial\mathcal{H}}{\partial\rho} + \lambda_t\right)\delta\rho\right\}dt + \int_0^T \frac{\partial\mathcal{H}}{\partial\varepsilon}\delta\varepsilon\, dt, \tag{A3}$$

where we have used $\delta\rho(0)=0$, since ρ is fixed at initial time. For an extremum, $\delta\bar{J}$ must be zero for arbitrary $\delta\varepsilon(t)$, $\delta\rho(t)$, and $\delta\rho(T)$. So, the adjoint equation

$$\lambda_t = -\frac{\partial\mathcal{H}(\rho(t),\varepsilon(t),\lambda(t))}{\partial\rho(t)}, \tag{A4}$$

with the initial condition $\lambda(T)=\Phi'_o(\rho(T))$ and the optimally condition

$$\frac{\partial\mathcal{H}(\rho(t),\varepsilon(t),\lambda(t))}{\partial\varepsilon} = 0, \tag{A5}$$

must hold.

[1] M. A. Nielson and I. L. Chuang, *Quantum Computation and Quantum Information* (Cambridge University Press, Cambridge, UK, 2000).
[2] C. H. Bennett, Phys. Today **48** (10), 24 (1995).
[3] H. M. Wiseman and A. C. Doherty, Phys. Rev. Lett. **94**, 070405 (2005).
[4] A. Barenco, T. A. Brun, R. Schack, and T. Spiller, e-print quant-ph/9612047.
[5] A. Bartana, R. Kosloff, and D. J. Tannor, Chem. Phys. **267**, 195 (2001).
[6] C. P. Koch, J. P. Palao, R. Kosloff, and F. Masnou-Seeuws, Phys. Rev. A **70**, 013402 (2004).
[7] A. E. Bryson and Y. C. Ho, *Applied Optimal Control* (Hemisphere, New York, 1975).
[8] A. P. Peirce, M. A. Dahleh, and H. Rabitz, Phys. Rev. A **37**, 4950 (1988).
[9] S. E. Sklarz and D. J. Tannor, Phys. Rev. A **66**, 053619 (2002).
[10] U. Hohenester, e-print cond-mat/0406346; U. Hohenester and G. Stadler, Phys. Rev. Lett. **92**, 196801 (2004).
[11] A. I. Solomon and S. G. Schirmer, e-print quant-ph/0401094.
[12] V. F. Krotov, *Global Methods in Optimal Control Theory* (Dekker, New York, 1996).
[13] K. G. Kim and M. D. Girardeau, Phys. Rev. A **52**, R891 (1995).
[14] S. G. Schirmer, M. D. Girardeau, and J. V. Leahy, Phys. Rev.

A **61**, 012101 (2000).
[15] V. S. Malinovsky and D. J. Tannor, Phys. Rev. A **56**, 4929 (2002).
[16] A. Borzi, G. Stadler, and U. Hohenester, Phys. Rev. A **66**, 053811 (2002).
[17] G. Lindblad, Commun. Math. Phys. **48**, 119 (1976).
[18] L. S. Pontriyagin *et al.*, *The Mathematical Theory of the Optimal Process* (Interscience, New York, 1962).
[19] J. T. Betts, *Practical methods for Optimal Control using Nonlinear Programming* (SIAM, Philadelphia, 2001).
[20] G. H. Golub and C. Van Loan, *Matrix Computations*, 2nd Edition (John Hopkins University Press, Balitimore and London, 1989).
[21] J. F. Frédéric, J. Ch. Gilbert, C. Lemaréchal, and C. Sagastizabál, *Numerical Optimization: Theoretical and Practical Aspects* (Springer, Heidelberg, 2003).
[22] W. H. Press, S. A. Teukolsky, W. T. Vertterling, and B. P. Flannery, *Numerical Recipes*, 2nd Edition (Cambridge University Press, Cambridge England, 1992).
[23] E. Hairer, S. P. Norsett, and G. Wanner, *Solving Ordinary Differentiel Equations. I. Nonstiff Problems* (Springer-Verlag, New York, 1993).
[24] H. P. Breuer and F. Petruccione, *The Theory of Open Quantum Systems* (Oxford University Press, New York 2002).
[25] Z. Haba and H. Kleinert, Eur. Phys. J. B **21**, 553 (2001).
[26] F. Rossi, eprint cond-mat/9711187.
[27] W. Pötz, Physica E (Amsterdam) **7**, 159 (2000).
[28] *Coherent Control in Atoms, Molecules, and Semiconductors*, edited by W. Pötz and W. Schroeder (Kluwer, Dordrecht, 1999).
[29] L. Viola and S. Lloyd, Phys. Rev. A **58**, 2733 (1998).
[30] L. Viola, E. Knill, and S. Lloyd, Phys. Rev. Lett. **82**, 2417 (1999).
[31] L. Faoro and L. Viola, Phys. Rev. Lett. **92**, 117905 (2004).
[32] D. Vitali and P. Tombesi, Phys. Rev. A **65**, 012305 (2002).
[33] N. V. Vitanov, M. Fleischhauer, B. W. Shore, and K. Bergmann, Adv. At., Mol., Opt. Phys. **46**, 55 (2001).
[34] N. V. Vitanov, T. Halfmann, B. W. Shore, and K. Bergmann, Annu. Rev. Phys. Chem. **52**, 763 (2001).
[35] P. A. M. Dirac, Proc. Cambridge Philos. Soc. **26**, 376 (1930).
[36] R. Balian and M. Veneroni. Phys. Rev. Lett. **47** 1353 (1981).
[37] G. L. Eyink, Phys. Rev. E **54**, 3419 (1996).